



**HAL**  
open science

## **Nuclear medicine for photodynamic therapy in cancer: planning, monitoring and nuclear PDT**

Dris Kharroubi Lakouas, Damien Huglo, Serge Mordon, Maximilien  
Vermandel

► **To cite this version:**

Dris Kharroubi Lakouas, Damien Huglo, Serge Mordon, Maximilien Vermandel. Nuclear medicine for photodynamic therapy in cancer: planning, monitoring and nuclear PDT. Photodiagnosis and Photodynamic Therapy, 2017, Epub ahead of print. 10.1016/j.pdpdt.2017.03.002 . inserm-01492527

**HAL Id: inserm-01492527**

**<https://inserm.hal.science/inserm-01492527>**

Submitted on 20 Mar 2017

**HAL** is a multi-disciplinary open access archive for the deposit and dissemination of scientific research documents, whether they are published or not. The documents may come from teaching and research institutions in France or abroad, or from public or private research centers.

L'archive ouverte pluridisciplinaire **HAL**, est destinée au dépôt et à la diffusion de documents scientifiques de niveau recherche, publiés ou non, émanant des établissements d'enseignement et de recherche français ou étrangers, des laboratoires publics ou privés.

# **Nuclear medicine for photodynamic therapy in cancer: planning, monitoring and nuclear PDT**

DrisKharroubiLakouas, MD,<sup>1,2</sup>, Damien Huglo, MD, PhD,<sup>1,2</sup>, Serge Mordon, PhD,<sup>1</sup>, Maximilien Vermandel, PhD,<sup>1,2</sup>

<sup>1</sup>Univ. Lille, Inserm, CHU Lille, U1189 - ONCO-THAI - Image Assisted Laser Therapy for Oncology, F-59000 Lille, France

<sup>2</sup>CHU Lille, Nuclear Medicine Department, F-59000, Lille, France

**Corresponding author:** m-vermandel@chru-lille.fr

**Abstract:** Photodynamic therapy (PDT) is a modality with promising results for the treatment of various cancers. PDT is increasingly included in the standard of care for different pathologies. This therapy relies on the effects of light delivered to photosensitized cells. At different stages of delivery, PDT requires imaging to plan, evaluate and monitor treatment. The contribution of molecular imaging in this context is important and continues to increase. In this article, we review the contribution of nuclear medicine imaging in oncology to PDT for planning and therapeutic monitoring purposes. Several solutions have been proposed to plan PDT from nuclear medicine imaging. For instance, photosensitizer biodistribution has been evaluated with radiolabeled photosensitizer or with conventional radiopharmaceuticals on positron emission tomography. The effects of PDT delivery have also been explored with specific SPECT or PET radiopharmaceuticals to evaluate the effects on cells (apoptosis, necrosis, proliferation, metabolism) or vascular damage. Finally, the synergy between photosensitizers and radiopharmaceuticals has been studied considering the Cerenkov effect to activate photosensitized cells.

**Keywords:** Photodynamic therapy, Oncology, PET, SPECT, 5-Aminolevulinic acid, PPIX

**Compliance with ethical standards**

**Conflicts of interest:** None

**Funding:** None

**Ethical approval:** This article does not contain any studies with human participants or animals performed by any of the authors.

## 1. Introduction

Photodynamic therapy (PDT) is a promising strategy for cancer therapy<sup>1,2</sup>. PDT is a non-thermal treatment based on the synergy of three elements: the administration of a photosensitizer drug; light at a precise wavelength; and the presence of oxygen (Figure 1). When these three components are combined, they lead to the formation of reactive oxygen species, resulting in a complex cascade of events and subsequent cell death, mainly via cytotoxic and vasculotoxic activity.

Most of the time, PDT relies on a specific biodistribution of a photosensitizer drug to tumor cells. Among photosensitizer drugs, porphyrins are the most frequently used in the literature<sup>3,4</sup>.

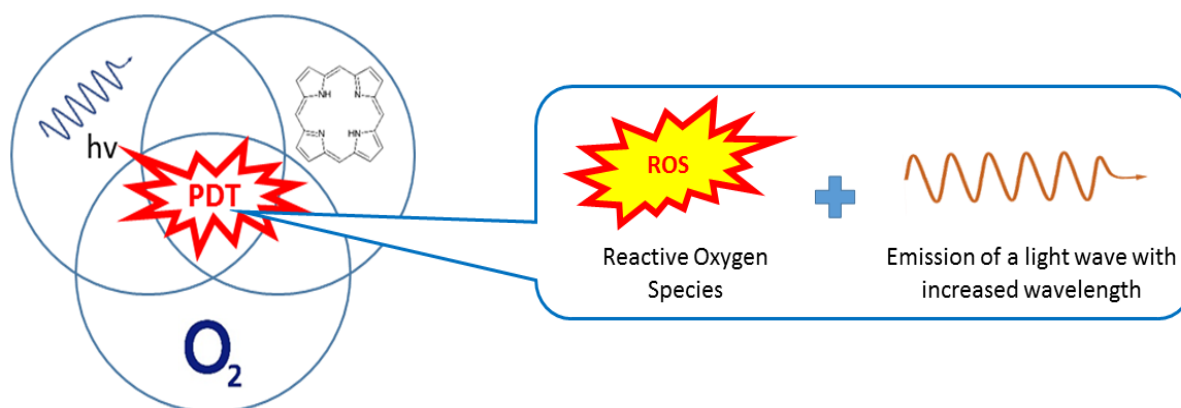


Figure 1: Illustration of the PDT mechanism, which is initiated by the combination of a photosensitizer, a light wave, and oxygen. PDT activation produces cytotoxic effects and fluorescence emission.

Porphyrins are macrocyclic organic compounds that have been implicated in various biological functions; the most common porphyrins are heme and chlorophyll. In addition to their interesting biological functions, they have high intrinsic specificity for tumors, low toxicity and favorable photophysical properties, such as fluorescence (Figure 1)<sup>5</sup>.

PDT was initially developed for dermatological lesions, which are easily accessible to light and can be monitored by visual assessment. Based on the success of this method and despite the low penetration of light in biological tissues, a promising method has been reported for the treatment of deep tumors using in situ inserted optical fibers<sup>6,7</sup>. This method is referred to as interstitial photodynamic therapy (iPDT). Therefore, to assess the photosensitizer biodistribution and monitor the therapeutic response of deep tumors, imaging is essential. Molecular imaging is a promising and prime candidate for PDT planning and monitoring, and the photosensitizer biodistribution is a relevant issue for PDT planning that radiolabeled photosensitizers or conventional PET radiopharmaceuticals may address efficiently. Molecular imaging also plays a key role in the monitoring of PDT. Radiotracers currently in use for molecular imaging may have applications in the evaluation of PDT effects, such as apoptosis, hypoxia, perfusion or mitochondrial viability.

This article aims to present the increasing contribution of nuclear medicine imaging in oncology for the planning and monitoring of PDT and the therapeutic prospects of nuclear PDT.

## 2. Photosensitizer biodistribution for photodynamic therapy planning

PDT relies on photosensitizer accumulation in a tumor, and some issues must be addressed prior to delivering treatment. Tumors may not have sufficient photosensitizer uptake to enable PDT<sup>8,9</sup>, or the drug accumulation may be heterogeneous. To address these issues and provide treatment planning solutions,

both the design of radiolabeled photosensitizers and molecular radiotracers already in use clinically are relevant.

#### **a. Radiolabeled porphyrins**

Porphyrins can be radiolabeled via simple complexation chemistry with their metallo-complex chelators as interesting biomarkers for in vivo quantitative biodistribution<sup>5</sup>. Radiolabeling of porphyrins was first achieved with copper-64 in 1951<sup>10,11</sup>. Hydrogen-3, carbon-14, palladium-109, sulfur-35, zinc-65, cobalt-57, and iodine-125 have also been explored but are unsuitable for in vivo imaging because of their long half-lives or weak gamma photon energy. For scintigraphic imaging, neodymium-104, gallium-67, indium-111 and technetium-99m (99mTc), the most commonly used isotope, have been evaluated<sup>12-21</sup>. For positron emission tomography imaging, radiolabeling with iodine-124, copper-64 and zinc-62 have been studied extensively<sup>5,10,22-27</sup>. In general, radiolabeled porphyrins accumulate in the tumor as standard porphyrins without altering the main characteristics of the host porphyrin molecules. Consequently, labeling using metal complexes of porphyrins is the most promising method<sup>5</sup>. A new metal isotope well-suited for human PET imaging, gallium-68, is now readily available. Based on the simple complexation chemistry with the porphyrin core and inexpensive germanium-68/gallium-68 radionuclide generator system, this isotope might become the prime isotope for radiolabeling porphyrins<sup>28-31</sup>. Unfortunately, despite several proposals for personalized planning of PDT<sup>1,5,12,19,20</sup>, radiolabeled porphyrins have not been studied for the prediction or quantitative assessment of photosensitizer uptake, probably because, until recently, PDT was limited to superficial tumors in which photosensitizer uptake is assessable by visual fluorescence. However, a commercialized photosensitizer for PDT, such as Photosan-3® (Seehof Laboratorium F&E GmbH, Wesselburenkoog, Germany), successfully radiolabeled<sup>12,21</sup> with 99m-technetium might be evaluated to individualize PDT treatment protocols.

#### **b. Photosensitizer prodrug: the case of 5-aminolevulinic acid**

5-Aminolevulinic acid (5-ALA) is a prodrug compound that is biologically inactive and preferentially accumulates in tumor cells, where it is transformed into protoporphyrin IX (PpIX) with a high tumor/surrounding healthy tissue ratio, particularly for glioblastoma. Hence, 5-ALA induces the selective accumulation of PpIX in tumor tissues. Consequently, 5-ALA is mainly used in clinical practice for fluorescence-guided resection of glioma to facilitate more complete resection compared with conventional surgery<sup>32</sup>. Objective responses have been observed for the treatment of non-melanoma skin cancer, gastrointestinal adenocarcinoma, bladder cancers, and glioma with PDT using 5-ALA<sup>2,9,33</sup>. Despite the high intrinsic specificity of PpIX for tumors, PpIX may be absent from the tumor or distributed heterogeneously, and an accurate assessment of PpIX accumulation is expected to predict PDT efficacy. Although fluorescence imaging is ideal to assess the presence of PpIX after 5-ALA administration, it is not always achievable for deep tumors. In response, radiolabeled 5-ALA compounds were recently developed. 5-Amino-4-oxo-[6-<sup>11</sup>C]hexanoic acid (11C-MALA) can be used to evaluate the quantitative accumulation and spatial distribution of 5-ALA in tumor tissues<sup>9,34</sup>, and for improved clinical availability, 99m-technetium-5-aminolevulinic acid was synthesized<sup>33</sup>. However, the potential correlation between the tumor biodistribution of 5-ALA and PpIX remains unclear and warrants further study.

#### **c. Common PET radiopharmaceuticals**

For certain pathologies, molecular imaging is more suitable to define tumor volume than conventional imaging, especially for neurosurgery or radiotherapy<sup>35-37</sup>. For example, PDT planning including 18F-fluorodeoxyglucose PET (18F-FDG PET) has been proposed for head and neck cancers<sup>38</sup>. However, very few studies have compared the accumulated amount of photosensitizer drug

as a function of the target volume defined by PET imaging. Studies comparing gadolinium-diethylenetriaminepentaacetic acid (Gd-DTPA) in Magnetic Resonance Imaging (MRI), 18F-fluoroethyl-L-tyrosine (18F-FET) PET, and 5-ALA tumor biodistribution for glioma, glioblastoma and meningioma<sup>8,39-42</sup> have demonstrated that metabolic imaging with 18F-FET is superior to Gd-DTPA enhancement in MRI for predicting the distribution of 5-ALA in glioblastoma, with a very high accuracy of 96% and a negative predictive value of 100%<sup>8,39</sup>. Thus, 18F-FET PET is an important tool for PDT in the brain, where the local fluorescence of PpIX cannot be observed. However, no study has compared the tumor distribution of 5-ALA to that of 3,4-dihydroxy-6-<sup>18</sup>F-fluoro-L-phenylalanine (18F-FDOPA), although the latter exhibits a better ratio of brain tumor/healthy tissue with Carbidoopa premedication than 18F-FET<sup>43</sup>. However, these studies also showed that the accuracy of 18F-FET to predict the 5-ALA tumor distribution decreased for low-grade glioma. These results are not due to the failure of 18F-FET PET but confirm that 5-ALA and porphyrins in general are sensitive to tumor grade<sup>8</sup>. Porphyrin accumulation depends on the type of cancer and especially on the degree of differentiation<sup>9,44</sup>. For gliomas, 18F-FET quantitative accumulation is correlated with tumor grade, and 18F-FDG accumulation is inversely correlated to tumor differentiation. For high-grade and dedifferentiated tumors, the glucose metabolism observed on 18F-FDG PET may be correlated with photosensitizer accumulation. In this context, an *in vitro* study demonstrated that 18F-FDG uptake before PDT can predict treatment efficacy<sup>45</sup>. This last point deserves further exploration.

### 3. Photodynamic therapy monitoring

Monitoring is required to evaluate the treatment response. In the early stage, monitoring enables adaptation of delivery in case of an inadequate response or the prediction of long-term response. Monitoring is generally accomplished using specific biomarkers to estimate the evolution of the disease. Tumor fluorescence can be considered a biomarker for monitoring treatment response when considering superficial tumors. However, as for the study of the biodistribution of photosensitizer drugs, fluorescence cannot be used for deep tumors. Several studies have proposed to address this problem by including metabolic imaging in PDT protocols to provide biomarkers and prognostic factors to predict treatment response earlier than morphological imaging<sup>1,5,19,20</sup>.

Radiolabeled porphyrins for monitoring after PDT have been suggested but have not been investigated further<sup>1,5,19,20</sup>. The main drawback might be the loss of sensitivity after treatment because tumor cells selected by PDT will no longer accumulate the photosensitizer. Consequently, monitoring using non-specific radiotracers seems more appropriate and convenient.

PDT induces a selective tumor response through different mechanisms. The effectiveness and preponderance of certain mechanisms compared to others is influenced by the illumination protocol, including the fluence and fractionation, by tissue oxygenation, and, obviously, by the type of photosensitizer drug<sup>2,46</sup>. The main mechanisms are impairment of tumor vascularization and direct cell death by apoptosis and necrosis. Therefore, different PDT effects may be observed with different radiotracers. The radiotracers presented in the following are of interest for monitoring PDT. These data are from preclinical studies and depend on the tumor models and therapeutic protocols (Table 1).

#### a. Glucose metabolism with 18F-fluorodesoxyglucose

The glucose analogue 18F-FDG enters tumor cells via the overexpressed membrane transporter GLUT and accumulates by phosphorylation in the cytoplasm. This very common radiopharmaceutical can be used to observe both tissue perfusion in minutes following intravenous administration and glucose metabolism in an equilibrium state (a minimum of 15 min post injection). When used after PDT, 18F-FDG PET shows the treatment response earlier than morphological imaging. As early as 30 minutes and 2 h after PDT, clear decreases in tumor perfusion and glucose metabolism due to the destruction of the

vascular system and direct cell death<sup>47,48</sup> were observed. At 24 and 48 h after PDT, 18F-FDG PET imaging showed, in most cases, a decrease in tumor metabolism<sup>48,49</sup>. Although one study showed an increase in tumor metabolic activity 24 h after PDT, the type of photosensitizer drug used might be responsible for this increase. The authors suggested hypermetabolism of the photosensitizer drug, a porphyrin-monoclonal antibody conjugate, at 24 h post-PDT via a probable acute inflammatory response<sup>49</sup>. Finally, 36 h after PDT, the metabolic volume on 18F-FDG PET described the absolute volume of the surviving tumor histological mass at a resolution similar to that of MRI, revealing the early extended injury caused by PDT<sup>50</sup>.

#### **b. Protein metabolism with 18F-fluoroethyltyrosine and 18F-fluorodihydroxyphenylalanine (18F-FDOPA)**

The radiolabeled amino acids 18F-FET and 18F-fluorodihydroxyphenylalanine (18F-DOPA) are mainly used for studies of brain tumors, in which these amino acids accumulate with excellent contrast compared to that in healthy tissue thanks to their ability to freely cross the blood-brain barrier and the overexpression of LAT transporters by tumor cells. No study has described the monitoring of PDT with these radiopharmaceuticals, but these amino acids are of particular interest for monitoring other treatments, especially for brain tumors. 18F-DOPA and 18F-FET are used for brain tumors in clinical practice by default with MRI, particularly to differentiate tumor progression from radionecrosis after glioma radiotherapy. Thus, radiolabeled amino acids could certainly be used to differentiate tumor progression from the tumor photonecrosis induced by PDT.

#### **c. Tumor proliferation with 18F-fluorodeoxythymidine**

18F-fluorodeoxythymidine (18F-FLT), a thymidine analogue, is trapped in cells and is phosphorylated by the cytosolic thymidine kinase-1, an enzyme of the pyrimidine salvage pathway of DNA synthesis. This radiopharmaceutical enables imaging of tumor proliferation. In two studies, 18F-FLT PET showed an early response to treatment with clear hypometabolism 4 h and 24 h after PDT<sup>51,52</sup>. Interestingly, after PDT, the decrease in metabolic proliferative activity observed using 18F-FLT PET appears to be more pronounced than the decreased metabolism glucose activity observed by 18F-FDG PET<sup>51</sup>.

#### **d. Membrane renewal with 11C-choline**

The phosphorylation of choline is catalyzed by choline kinase, which is overexpressed in tumor cells. Phosphorylcholine is incorporated into phosphatidylcholine, a component of the cell membrane. Thus, choline radiolabeling permits imaging of tumor membrane renewal. There is interest in following the early response of prostate cancer to PDT. From 1 to 48 h after therapy, PET imaging with 11C-choline revealed a marked decrease in tumor 11C-choline uptake<sup>53,54</sup>. 11C-Choline has not been studied in PDT monitoring for other cancers, and the radiolabeled forms with fluorine-18 (18F-fluoromethylcholine and 18F-fluoroethylcholine) have not been studied either.

#### **e. Apoptosis, 64-Cu-DOTA-biotin-Sav and 99-mTc-Annexin V**

Apoptosis is a mechanism of cell death induced by PDT and occurs very early, within the first hour following PDT<sup>2</sup>. Because it is tolerated better due to less tissue inflammation, apoptosis is the preferred cell death mechanism when choosing the photosensitizer drug and lighting method for PDT protocols. There are radiotracers for the apoptosis target phosphatidylserine, which is externalized by apoptotic cells. PET imaging using 64Cu-DOTA-biotin-Sav showed clear uptake within hours following PDT, from 4.5 h post-PDT. The amount of time to reach optimal contrast after PDT depends on the type of photosensitizer drug used and ranges from 6-7 h to 10-11 h post-PDT for two different photosensitizer drugs. However, the laborious protocol required prior to the injection of the radiotracer, which includes pretargeting with biotinylated annexin V, followed by an avidin chase to eliminate free biotinylated products, is an important drawback of the use of this radiopharmaceutical.

Moreover, the isotope 64-copper does not have ideal properties for diagnostic use in humans<sup>55</sup>. Another apoptosis radiotracer used in SPECT imaging, 99m-Tc-Annexin V, was tested for PDT. 99m-Tc-Annexin V might be well-suited for clinical use because it can be easily prepared within the clinical department of nuclear medicine, does not require pretargeting steps, and is perfectly suited for human use. Excellent uptake of 99mTc-Annexin V was observed in treated tumors 2, 4 and 7 h after PDT, as confirmed by histology<sup>56</sup>.

#### f. Hypoxia with 123I-iodoazomycin arabinoside

Although more recent PET radiotracers of hypoxia are available, 123I-iodoazomycin arabinoside (123I-IAZA) is the only radiotracer that has been studied for post-PDT monitoring. 123I-IAZA is metabolically reduced in viable cells and is inversely proportional to the intracellular oxygen concentration. 123I-IAZA exhibits significant accumulation 24h after PDT, concordant with a decrease in tissue perfusion<sup>57</sup>.

#### g. Perfusion and mitochondrial viability with 99mTc-hexakis-2-methoxyisobutyl isonitrile or 99mTc-hexamethylpropyleneamine oxime

The cationic complex 99mTc-hexakis-2-methoxyisobutyl isonitrile (99mTc-MIBI) is retained by the mitochondria mainly due to its lipophilicity and charge. The uptake of 99mTc-MIBI depends on the mitochondrion membrane potential and thus reflects mitochondrial viability. This complex was initially developed to visualize myocardial perfusion using scintigraphic imaging. The use of 99mTc-MIBI to assess tumor vascular perfusion after PDT revealed that tumor vascular perfusion decreased dramatically during the 2-h period following PDT and continued to decrease to 7% of the control value 24h later<sup>58,59</sup>. Another radiopharmaceutical for perfusion is 99mTc-hexamethylpropyleneamine oxime (99mTc-HMPAO), a liposoluble molecule that diffuses into the cell and then becomes hydrophilic and remains trapped in the cytoplasm. Tumor perfusion can be assessed to evaluate the vascular damage mechanism of PDT. Monitoring of PDT with 99mTc-HMPAO revealed maximal shut-down 8h post treatment, which persisted for at least 24h<sup>57,60</sup>. Regardless of tissue perfusion, 99mTc-MIBI is particularly interesting because some photosensitizers, such as Photofrin®, target the mitochondria. Therefore, 99mTc-MIBI does reveal destruction of mitochondria by the free radicals produced by PDT. The role of the mitochondria in the apoptosis mechanism could explain the apoptotic action of PDT. Accordingly, an in vitro study demonstrated that 99mTc-MIBI is superior to 18F-FDG for monitoring PDT, demonstrating a linear correlation with cell viability<sup>45</sup>.

Author	Radiotracer	Tumor histology	Photosensitizer	Effect evaluated	Time to significant effect	Model
D. Lapointe et al. 1999 <sup>47</sup>	Bolus <sup>18</sup> F-FDG	EMT6 murine mammary	PII and AlPcS	Glucose metabolism	30min	Mice
A.T. Byrne et al. 2009 <sup>48</sup>	Bolus <sup>18</sup> F-FDG	13762 MAT B III rat mammary	ADMP06	Glucose metabolism	30min	Rats
K. Smith et al. 2010 <sup>49</sup>	Bolus <sup>18</sup> F-FDG	LoVohuman colon adenocarcinoma	Anti-CD104- isothiocyanato porphyrin conjugate	Glucose metabolism	24h	Mice

<b>M. Sugiyama et al. 2004<sup>51</sup></b>	<sup>18</sup> F-FLT <sup>18</sup> F-FDG	HeLa	ATX-S10(Na)	Proliferation Glucose metabolism	24h Not significant 24h post PDT	Mice
<b>AE. O'Connor et al. 2012<sup>52</sup></b>	<sup>18</sup> F-FLT	MDA-MB-231-TGL human mammary and U87-TGL human glioma	ADPM06	Proliferation	4h	Mice
<b>B. Fei et al. 2010<sup>53</sup></b>	<sup>11</sup> C-Choline	PC-3 and CWR22, two human prostate	Pc 4	Membrane renewal	24h	Mice
<b>B. Fei et al. 2009<sup>54</sup></b>	<sup>11</sup> C-Choline	PC-3 human prostate	Pc 4	Membrane renewal	48h	Mice
<b>N. Cauchon et al. 2007<sup>55</sup></b>	<sup>64</sup> Cu-DOTA-biotin-SAv	EMT6 murine mammary	ZnPcS2 and AlPcS2	Apoptosis	4.5h	Mice
<b>M. Subbarayan et al. 2003<sup>56</sup></b>	<sup>99m</sup> Tc-annexin V	RIF-1 murine fibrosarcoma	Pc 4	Apoptosis	2h	Mice
<b>RB. Moore et al. 1993<sup>57</sup></b>	<sup>123</sup> I-IAZA <sup>99m</sup> Tc-HMPAO	R3327-AT rat prostate	PII	Hypoxia Vascular damage	24h 24h	Rats
<b>WS. Chan et al. 1997<sup>58</sup></b>	<sup>99m</sup> Tc-MIBI	EMT6 murine mammary	AlPc, AlPcS21 and AlPcS2	Vascular damage	3h	Mice
<b>N. Brasseur et al. 1996<sup>59</sup></b>	<sup>99m</sup> Tc-MIBI	EMT6 murine mammary	PII	Vascular damage	Immediately post PDT	Mice
<b>RB. Moore et al. 1992<sup>60</sup></b>	<sup>99m</sup> Tc-HMPAO	R3327-AT and R3327-H rat prostate	PII	Vascular damage	8h	Rats

Table 1: Preclinical studies on monitoring PDT with radiopharmaceuticals.

#### 4. Real time photodynamic therapy monitoring with dynamic PET

A new promising method to study tumor response in real time has recently been proposed to detect transient changes in uptake during treatment. This method consists of PDT applied during a dynamic

PET study, with multiple short frames reconstructed from list-mode data and a slow continuous infusion of  $^{18}\text{F}$ -FDG. Because of the continuous infusion, the  $^{18}\text{F}$ -FDG concentration does not reach an equilibrium state, but its rate of increase is constant. Thus, the effects of the treatment are observed in real time based on the kinetics of the radiopharmaceutical<sup>48,61,62</sup>. As previously explained, PDT acts via different mechanisms depending on the photosensitizer drug type. The two main mechanisms are direct cell death and impairment of the tumor vascularization. These mechanisms can be distinguished by real-time dynamic PET (Figure 2). Thus, damage to tumor vascularization is characterized by a delayed drop in tumor uptake that remains significantly lower after illumination ends. Direct cell death is characterized by a rapid reduction of  $^{18}\text{F}$ -FDG uptake followed by rapid restoration to more than 80% of the initial rate after illumination ends. Interestingly, this new method has led to the discovery of a systemic response to PDT because control tumors shielded from light also showed reduced  $^{18}\text{F}$ -FDG uptake during the illumination phase<sup>61</sup>. However, other mechanisms might have affected the kinetics of  $^{18}\text{F}$ -FDG, such as apoptosis and the inflammatory response in the tumors. Selective apoptosis is a desired response to PDT, whereas inflammation is often a side effect. Recent studies have shown that a low-fluence illumination protocol is more effective and better tolerated thanks to a greater apoptotic process and less inflammation<sup>63,64</sup>. Dynamic PET during PDT might also be explored to compare the metabolic responses to low and high fluence rates but remains to be studied.

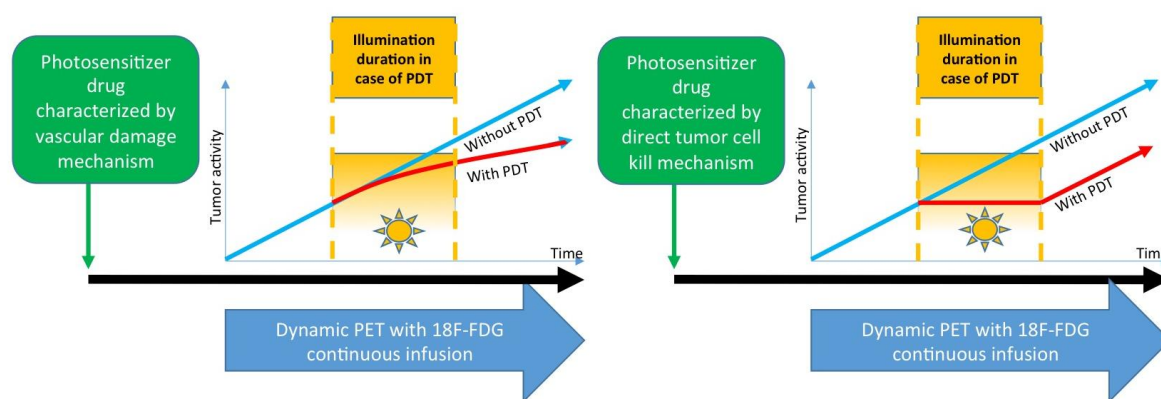


Figure 2: Illustration of the vascular damage mechanism and the direct tumor cell killing mechanism observed in real time by dynamic PET. On the left, the effect of PDT with a photosensitizer inducing vascular damage is characterized by a delayed drop in tumor uptake, followed by a long recovery period after the illumination ends. On the right, the effect of PDT with a photosensitizer inducing direct cell death is characterized by a rapid reduction in  $^{18}\text{F}$ -FDG uptake, followed by a rapid restoration after the illumination ends<sup>61</sup>.

## 5. Discussion and Perspectives

Molecular imaging might facilitate PDT planning by predicting the quantitative biodistribution of the photosensitizer in the tumor. In particular, a new metal isotope for PET imaging,  $^{68}\text{Ga}$ , offers easy radiolabeling using its metal complexes and holds promise for PDT planning<sup>5</sup>. Indeed, the simple complexation chemistry of  $^{68}\text{Ga}$  with the porphyrin core and good availability as the relatively low-cost  $^{68}\text{Ge}/^{68}\text{Ga}$  radionuclide generator system is highly suitable for radiolabeled porphyrins<sup>28-31</sup>. Given the importance of tumor oxygenation for the effectiveness of PDT, it is surprising that there has been no study of the ability of  $^{123}\text{I}$ -IAZA or other radiotracers of hypoxia to predict and follow the response to PDT. Imaging hypoxia prior to the delivery of PDT might be a key issue for adapting dosimetry (fractionation scheme, fluence rate, total dose).

However, radiolabeled porphyrins might not be suitable for monitoring the effect of PDT, and non-specific metabolic radiotracers might be preferable. The main mechanisms observed after PDT are damage to tumor vascularization and direct cell death caused by apoptosis and necrosis. Therefore,

different PDT effects maybe observed using different metabolic radiotracers routinely used in nuclear medicine.

Moreover, real-time  $^{18}\text{F}$ -FDG PET during PDT can assess PDT protocols in real time and thus enable optimization of their duration, oxygenation, and illumination to achieve personalized treatment. Consequently, monitoring PDT by dynamic PET could be a major advance in therapy. Thus, nuclear medicine, thanks to molecular imaging, offers interesting perspectives to optimize and personalize PDT.

However, the contribution of nuclear medicine is not limited only to PDT accompaniment but could also include PDT in deep tumors as an alternative to interstitial PDT. This so-called nuclear PDT relies on the Cherenkov effect as an alternative light source for PDT in deep tissue. Cherenkov radiation is an optical emission induced when charged particles move faster than the speed of light in a dielectric medium. This phenomenon is well known in the nuclear energy industry as it is responsible for the blue glow of an underwater nuclear reactor. The threshold energy of  $\beta$ -particles (electrons) to produce Cherenkov radiation in tissues is 0.219 MeV. High-energy photons can also indirectly produce Cherenkov radiation by secondary electrons caused by photoelectric interaction or Compton scattering<sup>65</sup>. Several isotopes used in radiopharmaceuticals emit particles with a greater energy than the threshold of 0.219 MeV and thus produce Cherenkov radiation<sup>66-68</sup>. Several recent studies have examined Cherenkov luminescence tomography, including in small animals<sup>69-71</sup>. Cherenkov radiation is of particular interest for PDT because it provides a deep light source without an invasive device. Cherenkov radiation is also perfectly adapted to PDT with 3 major benefits: proven efficacy and better tolerance of ultra-low fluence rate excitation during PDT<sup>63,72</sup>, with a meaningful effect at a 12 mJ/cm<sup>2</sup> threshold with a second-generation photosensitizer<sup>73</sup>; blue luminescence optimal for the activation of porphyrins<sup>1,74</sup> (Figure 3); and light production inside the tumor. In vivo photoactivation using Cherenkov from  $^{18}\text{F}$ FDG has been demonstrated as a proof of concept<sup>75</sup>, and tumor remission was achieved using a photosensitizer activated by Cherenkov radiation from radionuclides<sup>76,77</sup>. Isotopes with a longer half-life and emitting particles with greater energy, such as  $^{90}\text{Y}$ trium used in clinical oncology for the treatment of lymphoma (radioimmunotherapy with Zevalin®) and hepatocellular carcinoma (radioembolization with SirSpheres® or TheraSphere®), could deposit an adequate total Cherenkov light dose for PDT<sup>72</sup>. Thus, the synergy between internal radiotherapy and PDT warrants further investigation (Figure 4).

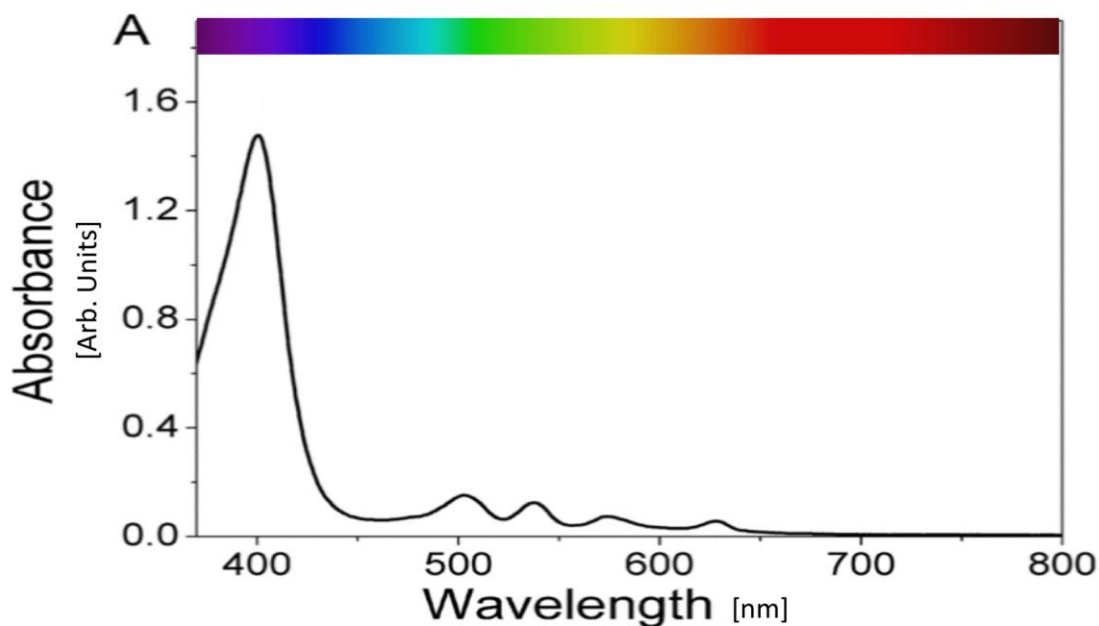


Figure 3: Absorption spectrum of protoporphyrin IX (PpIX).

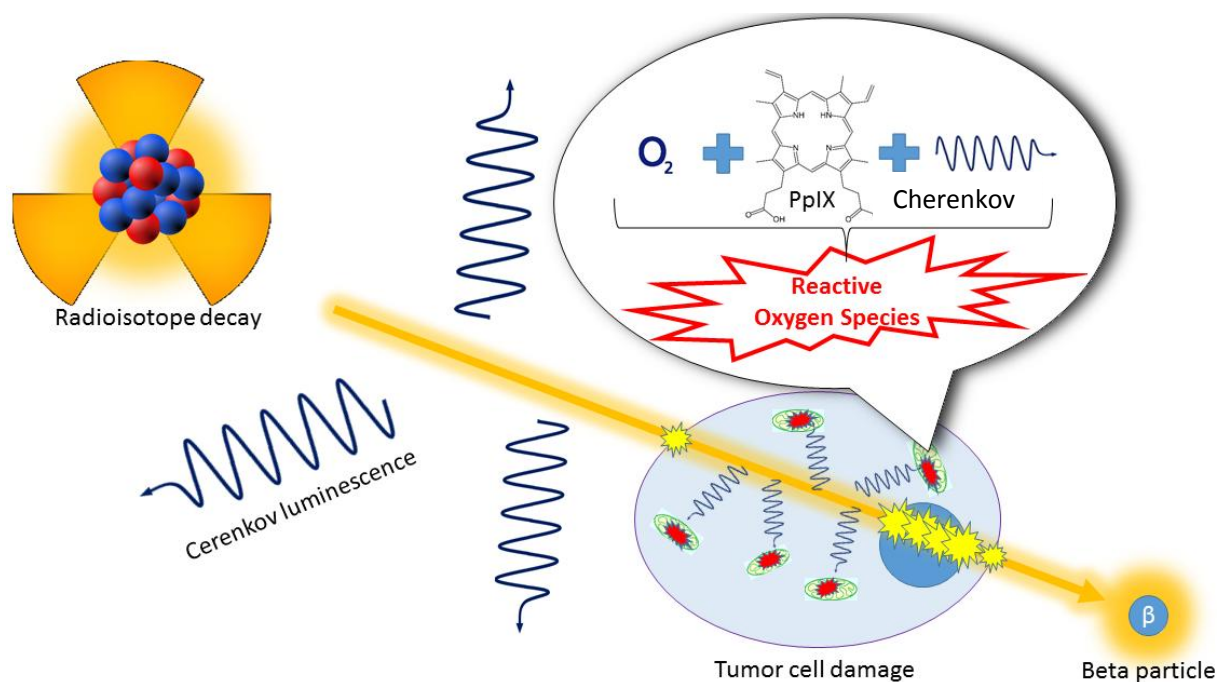


Figure 4: Illustration of nuclear PDT and the synergy between internal radiotherapy and photodynamic therapy.

## 6. Conclusion

Nuclear medicine is essential in oncology. It is an indispensable tool for a variety of current therapies and is also an asset for PDT. The simplicity and effectiveness of porphyrin radiolabeling, its low toxicity and its accumulation in tumor tissues make it a potential theranostic agent. The contribution of nuclear medicine is not limited to monitoring and might include the estimation of

photosensitizer uptake in deep tumors for improved treatment planning, the identification of various biological mechanisms of treatment and their effectiveness in real time, and as an optimal Cherenkov light source inside deep tumors.

## 7. References:

1. Josefsen LB, Boyle RW. Unique diagnostic and therapeutic roles of porphyrins and phthalocyanines in photodynamic therapy, imaging and theranostics. *Theranostics*. 2012;2(9):916-966. doi:10.7150/thno.4571.
2. Agostinis P, Berg K, Cengel K a, et al. Photodynamic Therapy of Cancer : An Update. *Am Cancer Soc*. 2011;61:250-281. doi:10.3322/caac.20114. Available.
3. Debele T, Peng S, Tsai H-C. *Drug Carrier for Photodynamic Cancer Therapy*. Vol 16.; 2015. doi:10.3390/ijms160922094.
4. Pushpan SK, Venkatraman S, Anand VG, et al. Porphyrins in photodynamic therapy - a search for ideal photosensitizers. *Curr Med Chem Anticancer Agents*. 2002;2(2):187-207. <http://www.ncbi.nlm.nih.gov/pubmed/12678743>.
5. Shi J. Transforming a Targeted Porphyrin Theranostic Agent into a PET Imaging Probe for Cancer. *Theranostics*. 2011:363. doi:10.7150/thno/v01p0363.
6. Bechet D, Mordon SR, Guillemin F, Barberi-heyob MA. Photodynamic therapy of malignant brain tumours : A complementary approach to conventional therapies. *Cancer Treat Rev*. 2014;40(2):229-241. doi:10.1016/j.ctrv.2012.07.004.
7. Quirk BJ, Brandal G, Donlon S, et al. Photodynamic therapy (PDT) for malignant brain tumors - where do we stand? *Photodiagnosis Photodyn Ther*. 2015:1-15. doi:10.1016/j.pdpdt.2015.04.009.
8. Floeth FW, Sabel M, Ewelt C, et al. Comparison of 18 F-FET PET and 5-ALA fluorescence in cerebral gliomas. *Eur J Nucl Med Mol Imaging*. 2011;38:731-741. doi:10.1007/s00259-010-1690-z.
9. Suzuki C, Tsuji AB, Kato K, et al. Preclinical Characterization of 5-Amino-4-Oxo-[6- 11 C] Hexanoic Acid as an Imaging Probe to Estimate Protoporphyrin IX Accumulation Induced by Exogenous Aminolevulinic Acid. *J Nucl Med*. 2015;55:1671-1678. doi:10.2967/jnumed.114.145086.
10. Waghorn P a. Radiolabelled porphyrins in nuclear medicine. *J Label Compd Radiopharm*. 2013;(October 2013). doi:10.1002/jlcr.3166.
11. Frank R . Wrenn , Myron L . Good PH. The Use of Positron-Emitting Radioisotopes for the Localization of Brain Tumors. *Science (80- )*. 1951;113(2940):525-527.
12. Babbar a. K, Singh a. K, Goel HC, Chauhan UPS, Sharma RK. Evaluation of 99mTc-labeled photosan-3, a hematoporphyrin derivative, as a potential radiopharmaceutical for tumor scintigraphy. *Nucl Med Biol*. 2000;27(6):587-592. doi:10.1016/S0969-8051(00)00123-2.
13. Maric N, Chan SM, Hoffer PB, Duray P. Radiolabeled porphyrin vs gallium-67 citrate for the detection of human melanoma in athymic mice. *Int J Rad Appl Instrum B*. 1988;15(5):543-551. doi:10.1016/S0969-8051(88)80013-1.
14. Foster N, Woo D V, Kaltovich F, Emrich J, Ljungquist C. Delineation of a transplanted malignant melanoma with indium-111-labeled porphyrin. *J Nucl Med*. 1985;26(7):756-760.
15. Robinson GD, Alavi a, Vaum R, Staum M. Imaging of lymph node uptake after intravenous administration of indium-111 metalloporphyrins. *J Nucl Med*. 1986;27(2):239-242.
16. Fazaeli Y, Jalilian AR, Amini MM, et al. Preparation and preliminary evaluation of [67Ga]-tetra phenyl porphyrin complexes as possible imaging agents. *J Radioanal Nucl Chem*.

- 2011;288(1):17-24. doi:10.1007/s10967-010-0962-1.
17. Aboudzadeh M, Fazaeli Y, Khodaverdi H, Afarideh H. Production, nano-purification, radiolabeling and biodistribution study of [140Nd] 5,10,15,20-tetraphenylporphyrin complex as a possible imaging agent. *J Radioanal Nucl Chem.* 2013;295(1):105-113. doi:10.1007/s10967-012-1826-7.
  18. Wang AY, Lin JL, Lin WC. Studies on the porphine labeled with 99mTc-pertechnetate. *J Radioanal Nucl Chem.* 2010;284:21-28. doi:10.1007/s10967-010-0466-z.
  19. Murugesan S, Shetty SJ, Srivastava TS, a.M Samuel, Noronha OPD. Preparation and biological evaluation of the new chlorin photosensitizer T3,4BCPC for detection and treatment of tumors. *J Photochem Photobiol B Biol.* 2002;68(1):33-38. doi:10.1016/S1011-1344(02)00329-9.
  20. Santos PM, Laranjo M, Serra AC, et al. Evaluation of a 99mTc-labelled meso-bisphenylporphyrin as a tumour image agent. *J Label Compd Radiopharm.* 2014;57(3):141-147. doi:10.1002/jlcr.3180.
  21. Whelan HT, Kras LH, Ozker K, et al. Selective incorporation of 111In-labeled PHOTOFRIN by glioma tissue in vivo. *J Neurooncol.* 1994;22(1):7-13. doi:10.1007/BF01058350.
  22. Bases R, Brodie SS, Rubinfeld S. Attempts at tumor localization using Cu 64-labeled copper porphyrins. *Cancer.* 1957;11:259-263.
  23. Ranyuk ER, Cauchon N, Ali H, Lecomte R, Guérin B, Van Lier JE. PET imaging using 64Cu-labeled sulfophthalocyanines: Synthesis and biodistribution. *Bioorganic Med Chem Lett.* 2011;21(24):7470-7473. doi:10.1016/j.bmcl.2011.09.121.
  24. Fazaeli Y, Jalilian AR, Amini MM, et al. Preparation, nano purification, quality control and labeling optimization of [64Cu]-5,10,15,20-tetrakis (penta fluoro phenyl) porphyrin complex as a possible imaging agent. *J Radioanal Nucl Chem.* 2013;295(1):255-263. doi:10.1007/s10967-012-1885-9.
  25. Tamura M, Matsui H, Hirohara S, et al. Selective accumulation of [62Zn]-labeled glycoconjugated porphyrins as multi-functional positron emission tomography tracers in cancer cells. *Bioorganic Med Chem.* 2014;22(8):2563-2570. doi:10.1016/j.bmc.2014.02.021.
  26. Chen Y, Sajjad M, Wang Y, Batt C, Nabi H a., Pandey RK. TSPO 18 kDa (PBR) targeted photosensitizers for cancer imaging (PET) and PDT. *ACS Med Chem Lett.* 2011;2:136-141. doi:10.1021/ml100211g.
  27. Pandey SK, Sajjad M, Chen Y, et al. Compared to Purpurinimides, the Pyropheophorbide Containing an Iodobenzyl Group showed Enhanced PDT Efficacy and Tumor Imaging (124I-PET) Ability. *Bioconjug Chem.* 2009;20(2):274-282. doi:10.1021/bc8003638.Compared.
  28. Bryden F, Savoie H, Rosca E V, Boyle RW. PET/PDT theranostics: synthesis and biological evaluation of a peptide-targeted gallium porphyrin. *Dalt Trans.* 2015;44(11):4925-4932. doi:10.1039/C4DT02949F.
  29. Zoller F, Riss PJ, Montforts FP, Kelleher DK, Eppard E, Rösch F. Radiolabelling and preliminary evaluation of 68Ga-tetrapyrrole derivatives as potential tracers for PET. *Nucl Med Biol.* 2013;40(2):280-288. doi:10.1016/j.nucmedbio.2012.11.006.
  30. Fazaeli Y, Jalilian AR, Amini MM, et al. Development of a 68Ga-Fluorinated Porphyrin Complex as a Possible PET Imaging Agent. *Nucl Med Mol Imaging (2010).* 2012;46(1):20-26. doi:10.1007/s13139-011-0109-5.
  31. Bhadwal M, Das T, Dev Sarma H, Banerjee S. Radiosynthesis and Bioevaluation of [68Ga]-Labeled 5,10,15,20-Tetra(4-methylpyridyl)-porphyrin for Possible Application as a PET Radiotracer for Tumor Imaging. *Mol Imaging Biol.* 2014;17(1):111-118. doi:10.1007/s11307-014-0760-1.

32. Stummer W, Pichlmeier U, Meinel T, Wiestler OD, Zanella F, Reulen HJ. Fluorescence-guided surgery with 5-aminolevulinic acid for resection of malignant glioma: a randomised controlled multicentre phase III trial. *Lancet Oncol.* 2006;7(5):392-401. doi:10.1016/S1470-2045(06)70665-9.
33. Khan KU, Roohi S, Rafi M, Zahoor R, Ahmad M. Evaluation of labelling conditions, quality control and biodistribution study of <sup>99m</sup>Tc-5-aminolevulinic acid (5-ALA): a potential liver imaging agent. *J Radioanal Nucl Chem.* 2014;300(1):225-228. doi:10.1007/s10967-014-3014-4.
34. Suzuki M, Takashima-Hirano M, Ishii H, et al. Synthesis of <sup>11</sup>C-labeled retinoic acid, [<sup>11</sup>C]ATRA, via an alkenylboron precursor by Pd(0)-mediated rapid C-[<sup>11</sup>C] methylation. *Bioorganic Med Chem Lett.* 2014;24(15):3622-3625. doi:10.1016/j.bmcl.2014.05.041.
35. Jelercic S, Rajer M. The role of PET-CT in radiotherapy planning of solid tumours. *Radiol Oncol.* 2015;49(1):1-9. doi:10.2478/raon-2013-0071.
36. Niyazi M, Geisler J, Siefert A, et al. FET-PET for malignant glioma treatment planning. *Radiother Oncol.* 2011;99(1):44-48. doi:10.1016/j.radonc.2011.03.001.
37. Nowosielski M, DiFranco MD, Putzer D, et al. An intra-individual comparison of MRI, [<sup>18</sup>F]-FET and [<sup>18</sup>F]-FLT PET in patients with high-grade gliomas. *PLoS One.* 2014;9(4). doi:10.1371/journal.pone.0095830.
38. Karakullukcu B, Van Veen RLP, Aans JB, et al. MR and CT based treatment planning for mTHPC mediated interstitial photodynamic therapy of head and neck cancer: Description of the method. *Lasers Surg Med.* 2013;45(August):517-523. doi:10.1002/lsm.22174.
39. Stockhammer F, Misch M, Horn P, Koch A, Fonyuy N, Plotkin M. Association of F18-fluoro-ethyl-tyrosin uptake and 5-aminolevulinic acid induced fluorescence in gliomas. *Acta Neurochir (Wien).* 2009;(151):1377-1383. doi:10.1007/s00701-009-0462-7.
40. Ewelt C, Floeth FW, Felsberg J, et al. Finding the anaplastic focus in diffuse gliomas : The value of Gd-DTPA enhanced MRI , FET-PET , and intraoperative , ALA-derived tissue fluorescence. *Clin Neurol Neurosurg.* 2011;113(7):541-547. doi:10.1016/j.clineuro.2011.03.008.
41. Cornelius JF, Steiger HJ, Stoffels G, Galldiks N, Langen KJ. 5-Aminolevulinic Acid and 18 F-FET-PET as Metabolic Imaging Tools for Surgery of a Recurrent Skull Base Meningioma. *J Neurol Surg Part B.* 2013;74:211-216.
42. Roessler K, Becherer A, Donat M, Cejna M. Intraoperative tissue fluorescence using 5-aminolevulinic acid (5-ALA) is more sensitive than contrast MRI or amino acid positron emission tomography (18F-FET PET) in glioblastoma surgery. *Neurol Res.* 2012;34(3):3-6. doi:10.1179/1743132811Y.0000000078.
43. Kratochwil C, Combs SE, Leotta K, et al. Intra-individual comparison of 18F-FET and 18F-DOPA in PET imaging of recurrent brain tumors. *Neuro Oncol.* 2014;16(3):434-440. doi:10.1093/neuonc/not199.
44. Valdés PA, Kim A, Brantsch M, et al.  $\delta\delta$ -aminolevulinic acid-induced protoporphyrin IX concentration correlates with histopathologic markers of malignancy in human gliomas: the need for quantitative fluorescence-guided resection to identify regions of increasing malignancy. *Neuro Oncol.* 2011;13(8):846-856. doi:10.1093/neuonc/nor086.
45. Liu J, Ogawa M, Sakai T, Takashima M, Okazaki S, Magata Y. Differentiation of tumor sensitivity to photodynamic therapy and early evaluation of treatment effect by nuclear medicine techniques. *Ann Nucl Med.* 2013;27(7):669-675. doi:10.1007/s12149-013-0734-4.
46. Tetard M-C, Vermandel M, Leroy H-A, et al. Interstitial 5-ALA photodynamic therapy and glioblastoma: Preclinical model development and preliminary results. *Photodiagnosis*

- Photodyn Ther.* 2016;13:218-224. doi:10.1016/j.pdpdt.2015.07.169.
47. Lapointe D, Brasseur N, Cadorette J, et al. High-resolution PET imaging for in vivo monitoring of tumor response after photodynamic therapy in mice. *J Nucl Med.* 1999;40:876-882.
  48. Byrne a T, O'Connor a E, Hall M, et al. Vascular-targeted photodynamic therapy with BF2-chelated Tetraaryl-Azadipyromethene agents: a multi-modality molecular imaging approach to therapeutic assessment. *Br J Cancer.* 2009;101:1565-1573. doi:10.1038/sj.bjc.6605247.
  49. Smith K, Malatesti N, Cauchon N, et al. Mono- and tri-cationic porphyrin-monoclonal antibody conjugates: Photodynamic activity and mechanism of action. *Immunology.* 2010;132:256-265. doi:10.1111/j.1365-2567.2010.03359.x.
  50. Moore J V, Waller ML, Zhao S, et al. Feasibility of imaging photodynamic injury to tumours by high-resolution positron emission tomography. *Eur J Nucl Med.* 1998;25(9):1248-1254. doi:10.1007/s002590050292.
  51. Sugiyama M, Sakahara H, Sato K, Harada N, Fukumoto D. Evaluation of 3'-Deoxy-3'-18 F Fluorothymidine for Monitoring Tumor Response to Radiotherapy and Photodynamic Therapy in Mice. *J Nucl Med.* 2004;45(45):1754-1758.
  52. O'Connor AE, Mc Gee MM, Likar Y, et al. Mechanism of cell death mediated by a BF 2-chelated tetraaryl-azadipyromethene photodynamic therapeutic: Dissection of the apoptotic pathway in vitro and in vivo. *Int J Cancer.* 2012;130:705-715. doi:10.1002/ijc.26073.
  53. Fei B, Wang H, Wu C, Chiu S. Choline PET for monitoring early tumor response to photodynamic therapy. *J Nucl Med.* 2010;51:130-138. doi:10.2967/jnumed.109.067579.
  54. Fei B, Wang H, Wu C, et al. Choline Molecular Imaging with Small animal PET for Monitoring Tumor Cellular Response to Photodynamic Therapy of Cancer. *Proc SPIE.* 2009;7262(726211). doi:10.1037/a0013262.Open.
  55. Cauchon N, Langlois R, Rousseau J a., et al. PET imaging of apoptosis with 64Cu-labeled streptavidin following pretargeting of phosphatidylserine with biotinylated annexin-V. *Eur J Nucl Med Mol Imaging.* 2007;34(2):247-258. doi:10.1007/s00259-006-0199-y.
  56. Subbarayan M, Häfeli UO, Feyes DK, Unnithan J, Emancipator SN, Mukhtar H. A simplified method for preparation of 99mTc-annexin V and its biologic evaluation for in vivo imaging of apoptosis after photodynamic therapy. *J Nucl Med.* 2003;44(4):650-656.
  57. Moore RB, Chapman JD, Mercer JR, et al. Measurement of PDT-induced hypoxia in Dunning prostate tumors by iodine-123-iodoazomycin arabinoside. *J Nucl Med.* 1993;34(3):405-411.
  58. Chan WS, Brasseur N, La Madeleine C, Ouellet R, Van Lier JE. Efficacy and mechanism of aluminum phthalocyanine and its sulfonated derivatives mediated photodynamic therapy on murine tumors. *Eur J Cancer.* 1997;33(11):1855-1859.
  59. Brasseur N, Lewis K, Rousseau J, van Lier JE. Measurement of tumor vascular damage in mice with 99mTc-MIBI following photodynamic therapy. *Photochem Photobiol.* 1996;64(4):702-706.
  60. Moore RB, Chapman JD, Mokrzanowski a D, Arnfield MR, McPhee MS, McEwan a J. Non-invasive monitoring of photodynamic therapy with 99technetium HMPAO scintigraphy. *Br J Cancer.* 1992;65(4):491-497.
  61. Bérard V, Rousseau J a, Cadorette J, et al. Dynamic imaging of transient metabolic processes by small-animal PET for the evaluation of photosensitizers in photodynamic therapy of cancer. *J Nucl Med.* 2006;47:1119-1126. doi:47/7/1119 [pii].
  62. Cauchon N, Turcotte E, Lecomte R, Hasséssian HM, Lier JE Van. Predicting efficacy of photodynamic therapy by real-time FDG-PET in a mouse tumour model. *Photochem {&} Photobiol Sci.* 2012;11(2):364. doi:10.1039/c1pp05294b.

63. Mathews MS, Angell-Petersen E, Sanchez R, et al. The effects of ultra low fluence rate single and repetitive photodynamic therapy on glioma spheroids. *Lasers Surg Med.* 2009;41(8):578-584. doi:10.1002/lsm.20808.
64. Lilge L, Portnoy M, Wilson BC. Apoptosis induced in vivo by photodynamic therapy in normal brain and intracranial tumour tissue. *Br J Cancer.* 2000;83(8):1110-1117. doi:10.1054/bjoc.2000.1426.
65. Thorek DL, Robertson R, Bacchus W a, et al. Cerenkov imaging - a new modality for molecular imaging. *Am J Nucl Med Mol Imaging.* 2012;2(2):163-173.
66. Gill RK, Mitchell GS, Cherry SR. Computed Cerenkov luminescence yields for radionuclides used in biology and medicine. *Phys Med Biol.* 2015;60(11):4263-4280. doi:10.1088/0031-9155/60/11/4263.
67. Liu H, Ren G, Miao Z, et al. Molecular optical imaging with radioactive probes. *PLoS One.* 2010;5(3). doi:10.1371/journal.pone.0009470.
68. Dothager RS, Goiffon RJ, Jackson E, Harpstrite S, Piwnica-Worms D. Cerenkov radiation energy transfer (CRET) imaging: A novel method for optical imaging of PET isotopes in biological systems. *PLoS One.* 2010;5(10):1-7. doi:10.1371/journal.pone.0013300.
69. Hu Z, Liang J, Yang W, et al. Experimental Cerenkov luminescence tomography of the mouse model with SPECT imaging validation. *Opt Express.* 2010;18(24):24441-24450. doi:10.1364/OE.18.024441.
70. Li C, Mitchell GS, Cherry SR. Cerenkov luminescence tomography for small-animal imaging. *Opt Lett.* 2010;35(7):1109-1111. doi:10.1364/OL.35.001109.
71. Zhong J, Tian J, Yang X, Qin C. Whole-body cerenkov luminescence tomography with the finite element SP 3 method. *Ann Biomed Eng.* 2011;39(6):1728-1735. doi:10.1007/s10439-011-0261-1.
72. Gonzales J, Wang F, Zamora G, et al. Ultra low fluence rate photodynamic therapy : Simulation of light emitted by the Cerenkov effect . *Proc os SPIE Opt Tech Neurosurgery, Neurophotonics, Optogenetics.* 2014;8928:1-11. doi:10.1117/12.2041631.
73. Hartl BA, Hirschberg H, Marcu L, Cherry SR. Characterizing low fluence thresholds for in vitro photodynamic therapy. *Biomed Opt Express.* 2015;6(3):770-779. doi:10.1364/BOE.6.000770.
74. Celli JP, Spring BQ, Rizvi I, et al. Imaging and Photodynamic Therapy: Mechanisms, Monitoring and Optimization. *Chem Rev.* 2011;110(5):2795-2838. doi:10.1021/cr900300p.Imaging.
75. Ran C, Zhang Z, Hooker J, Moore A. In vivo photoactivation without “light”: Use of cherenkov radiation to overcome the penetration limit of light. *Mol Imaging Biol.* 2012;14(2):156-162. doi:10.1007/s11307-011-0489-z.
76. Kotagiri N, Sudlow GP, Akers WJ, Achilefu S. Breaking the depth dependency of phototherapy with Cerenkov radiation and low-radiance-responsive nanophotosensitizers. *Nat Nanotechnol.* 2015;10(4):370-379. doi:10.1038/nnano.2015.17.
77. Hartl BA, Hirschberg H, Marcu L, Cherry SR. Activating Photodynamic Therapy in vitro with Cerenkov Radiation Generated from Yttrium-90. *J Environ Pathol Toxicol Oncol.* 2016;35(2):185-192. doi:10.1615/JEnvironPatholToxicolOncol.2016016903.